

A Measurement of the HRMA Vignetting with Abell 1795

Eli Beckerman, Diab Jerius

Smithsonian Astrophysical Observatory, 60 Garden Street, Cambridge, MA 02138

Abstract

We extend our calibration of the as-measured vignetting of the focal plane by the *Chandra* optics by analyzing an off-axis pointing of A1795, a galaxy cluster. The observation yielded data which are relatively bright, yet not piled up. Earlier measurements of telescope vignetting using G21.5-0.9 are complicated by pileup. We have performed a sensitivity analysis to determine the effect of the extended nature of A1795 on measurements of the vignetting. We present the results of this analysis as well as the determined vignetting value in the context of our previous findings.

Introduction

Earlier measurements of the HRMA vignetting¹ used a series of off-axis observations of the bright supernova remnant G21.5-0.9. Ideally vignetting measurements would be made with a bright point source, but we are limited by pileup as we must use ACIS for spectral sensitivity. Surface brightness ratios for G21.5, corrected for HRMA vignetting, actually showed values greater than unity, pointing toward either a pileup problem or an overestimate in the vignetting correction from the telescope models. Analysis of two ACIS “standard candles” by Alexey Vikhlinin², G21.5 and E0102, points to pileup as a problem in flux measurements of these two SNRs. The pileup fraction is as large as 5.4% for on-axis observations of G21.5. Vikhlinin³ also pointed out that on- and off-axis observations of the galaxy cluster Abell 1795 were available, and his preliminary analysis yielded corrected flux ratios of ~ 1 . Since the extended nature of the source adds complications to the vignetting analysis, we perform a sensitivity study to examine contamination from other parts of the source as the PSF broadens off-axis.

Observations

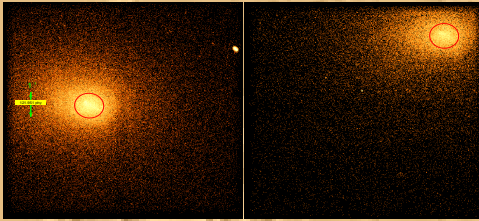


Figure 1: a) OBSID 5287, 1.035' off-axis, on ACIS-S3. b) OBSID 5290, 6.683' off-axis, on ACIS-I3. Source region to be an ellipse such that 1% of flux off-axis is from outside of the ellipse, as determined from raytraces.

We use two 15 ksec ACIS observations of Abell 1795 which are relatively bright and do not suffer from pileup. Unlike the observations of G21.5, the A1795 observations do not track the source with the SIM in order to minimize the QE differences. OBSID 5287, our on-axis observation, is actually 1.035' off-axis. The off-axis observation is OBSID 5290, and was taken 6.683' off-axis. This 6.7' observation places Abell 1795 in the corner of I3, so the raw count ratios are affected by QE differences between observations, especially at low energies due to the contamination of the ACIS OBF. We choose an ellipse for our source region such that 1% of the flux off-axis is scattered in from outside the ellipse, as determined by the raytraces.

Simulations & Analysis

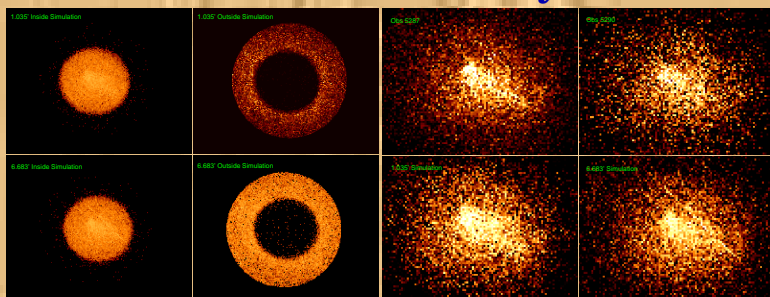


Figure 2: a) Inside and outside regions raytraced from 1.035' image, at $\theta=1.035'$ (top row) and $\theta=6.683'$ (bottom row). b) Comparison of observations (top row) to raytraced images (bottom row).

In order to determine how much of the flux in our source region is actually from the outer parts of the galaxy cluster, we split the cluster into two components, and raytraced these images independently using the *SAO* software. We assume that using a $\theta=1.035'$ observation for the baseline image to raytrace is appropriate to study how the source changes as it is moved further off-axis. We set the relative weights of the inside and outside regions by dividing the ratio of inside/outside flux for the observation by that of a raytrace with equal photon densities. Raytracing the inside and outside sources independently allows us to determine the relative contributions at a given position. We also combine the inside and outside raytraces to make direct comparisons to the observations.

In order to minimize the contamination from outer parts of the source yet maximize the amount of flux we get from the source, we choose an ellipse where 1% of the flux in the off-axis raytraces comes from the outside region. A line is drawn in Figure3a below to indicate this ellipse (63-pixel semi-major axis).

As in the previous analysis, we present 3 diagnostic ratios between the off- and on-axis observations. Two of these ratios include position- and energy-dependent corrections, for which we create exposure maps in given energy bands, weighted by a fit to the on-axis spectrum. The data are background subtracted using the standard ACIS background datasets, normalized by the high-energy (9.5-12 keV) counts in the observation.

- the raw counts ratio R_1 , which is the observed vignetting function, which includes all effects in the system (mirrors, support structures, detector non-uniformities, etc.)
- QE-corrected surface brightness ratio, R_2 . If the CALDB QE curves are correct, then this ratio is the telescope optical vignetting, which we assume to be pure HRMA vignetting.
- QE+EA corrected surface brightness ratio, R_3 , where EA is the HRMA effective area from the CALDB. Since these are corrected for all vignetting effects, this ratio would equal unity for an accurate vignetting correction.

$$R_1 = \frac{\Sigma_{a1} - \Sigma_{b1}}{\Sigma_{a0} - \Sigma_{b0}} = \frac{\left(\frac{N_{a1}}{A_{a1}} - \frac{N_{b1}}{A_{b1}}\right)}{\left(\frac{N_{a0}}{A_{a0}} - \frac{N_{b0}}{A_{b0}}\right)} \quad R_2 = \frac{\left(\frac{N_{a1}}{A_{a1}Q_{a1}t_1} - \frac{N_{b1}}{A_{b1}Q_{b1}t_1}\right)}{\left(\frac{N_{a0}}{A_{a0}Q_{a0}t_0} - \frac{N_{b0}}{A_{b0}Q_{b0}t_0}\right)} \quad R_3 = \frac{\left(\frac{N_{a1}}{A_{a1}Q_{a1}V_{a1}t_1} - \frac{N_{b1}}{A_{b1}Q_{b1}V_{b1}t_1}\right)}{\left(\frac{N_{a0}}{A_{a0}Q_{a0}V_{a0}t_0} - \frac{N_{b0}}{A_{b0}Q_{b0}V_{b0}t_0}\right)}$$

where Σ is the surface brightness, N is the number of counts, A is the area of the region, t is the effective exposure time, f is the background-scaling factor based on high-energy fluxes, and Q and V are the QE and vignetting corrections in the CALDB. Subscripts 0 and 1 denote on-axis and off-axis, respectively, while a and b refer to source versus background.

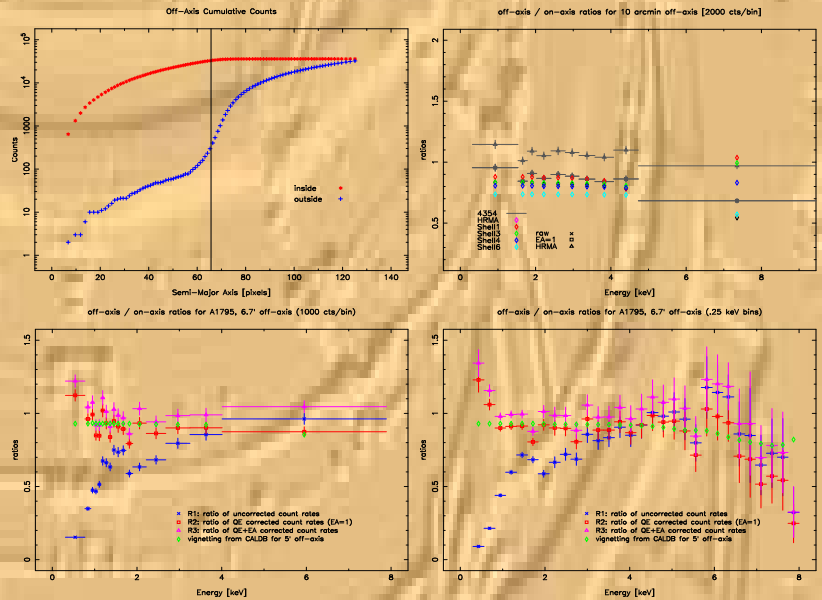


Figure 3: a) Cumulative counts for the off-axis raytraces showing the cut-off of our source region. b) Off-axis/On-axis surface brightness ratios for G21.5-0.9, $\theta=5'$. c) Surface brightness ratios for Abell 1795 (1000 counts per energy bin). d) Surface brightness ratios for Abell 1795 (0.25 keV energy bins).

Conclusions

QE variations between these two observations show up when the raw counts ratios and QE-corrected ratios, R_1 and R_2 respectively, are not in agreement with each other, as they were for G21.5. This is especially evident at low energies because of the contamination of the ACIS OBF. The QE+EA corrected ratios show that the HRMA vignetting in the CALDB is good to within 10% and shows some indication that the G21.5 measurements are affected by pileup, causing R_3 to be greater than 1. Future improvements to the vignetting measurement may include using larger source regions off-axis to track the growth of the PSF, ensuring that we are comparing consistent regions of the astrophysical source.

References

1. E. Beckerman, B. Biller, D. Jerius, “Measurement of Telescope Vignetting with SNR G21.5-0.9”, 2003 November 26, *Chandra Calibration Workshop* http://cxc.harvard.edu/ccw/proceedings/03_proc/presentations/beckerman/index.html
2. A. Vikhlinin, Pileup in the ACIS “standard candles”, 2004 April 4 <http://hea-www.harvard.edu/~alexey/acis/memos/pileup-e0102-g215.pdf>
3. A. Vikhlinin, *private communication*, 2004 April 8